

Chiral Skin Effect

Xin-Ran Ma,^{1,*} Kui Cao,^{1,*} Xiao-Ran Wang,¹ Zheng Wei,¹ and Su-Peng Kou^{1,†}

¹*Department of Physics, Beijing Normal University, 100875, Beijing*

Recently, the interplay between non-Hermitian effect and topological insulators becomes a hot spot and frontier of research in non-Hermitian physics. An interesting phenomenon is hybrid skin-topological effect that is a special type of non-Hermitian skin effect for topological protected edge states. Now, topological protected edge states become localized at certain corners, while the bulk states are still extended. However, the mechanism of hybrid skin-topological effect is still an open question. In this paper, this open question is completely solved. The key point is the discovery of an alternative type of non-Hermitian skin effect for dissipative chiral modes – chiral skin effect, i.e., Chiral modes + Dissipation \rightarrow Chiral skin effect. According to chiral skin effect, topological edge states on the dissipative edges of a 2D topological insulator become localized around the gain/loss boundaries, which separate the regions of gain and those of loss. By considering non-Hermitian two dimensional Haldane model with edge dissipation as an example, we show the detailed physical properties of chiral skin effect. An additional interesting phenomenon that is relevant chiral skin effect is non-local non-Hermitian skin effect, which causes the topological edge state of both sides to be localized only on the same gain/loss boundary. This progress will be helpful for the research on both non-Hermitian physics and topological quantum states.

Non-Hermitian quantum system has attracted intensive attention due to its rich underlying physics distinguishing from its Hermitian counterparts[1–10]. There are many interesting phenomena in non-Hermitian quantum systems, such as exceptional points(EP) and non-Hermitian skin effect(NHSE). *Exceptional point* is known as the non-Hermitian degeneracy, at which different wave functions merge into one[1, 11, 12]. In addition, *non-Hermitian skin effect* is another exotic effect in non-Hermitian systems[13–40]. For a non-Hermitian system with NHSE, the bulk states become exponentially localized around the boundaries of the system, and are characterized by generalized Brillouin zone (GBZ) rather than usual Brillouin zone (BZ)[13–15, 41].

Recently, the interplay of NHSE and topological insulator leads to varied, interesting physical effects, such as defective edge states[5, 16], non-Hermitian topological invariant[13, 20, 25, 29], and hybrid skin-topological effect[17, 18, 33]. *Hybrid skin-topological effect* is a special type of NHSE, of which topological protected edge/boundary states become localized at certain corners, while the bulk states are still extended. In other words, hybrid skin-topological effect is a NHSE for topological edge/boundary states. However, about the mechanism of hybrid skin-topological effect, there still exists *controversy*. In Ref.[17], it was pointed out that by considering the topological edge states as those on a one-dimensional chain, it originates from the interplay between gain, loss, and the chiral edge currents induced by the non-local flux. In Ref.[18], a class of hybrid skin-topological modes is attributed to higher-order non Hermitian skin effect.

In this paper, we reexamine this issue by studying a

topological insulator with edge/boundary dissipation. In particular, we point out that to explore the mechanism of hybrid skin-topological effect one *cannot* consider the topological edge states as those on a one-dimensional chain, and hybrid skin-topological effect *cannot* be regarded as a higher-order non Hermitian skin effect. Instead, we found that hybrid skin-topological effect is really a new type of NHSE – *chiral skin effect* (CSE) that can be regarded as a "fractional" NHSE. By taking non-Hermitian Haldane model with edge dissipation as an example, we show the detailed physical property of CSE.

Chiral skin effect. To study the intrinsic mechanism of hybrid topological skin effect, we first show the key properties of chiral skin effect for one dimensional (1D) dissipative chiral modes in continuous limit.

In continuous limit, the effective single-body Hamiltonian for 1D chiral modes in low-energy physics becomes

$$\hat{h}_{\text{edge}} = v \cdot \hat{k}, \quad (1)$$

where v is the velocity of edge states and \hat{k} is the momentum operator of the chiral modes. An example of chiral modes is topological edge states of a two dimensional topological insulator with edge dissipation. See the illustration in Fig.1(a).

Then, we consider the effect from dissipation, of which the strength is $\gamma(x)$. There is a notable aspect of chiral modes that *dissipation plays the role of imaginary wave vector*. Now, the effective Hamiltonian turns into

$$\hat{h}_{\text{edge}} = v \cdot \hat{k} + i\gamma(x). \quad (2)$$

In this case, we have an imaginary wave vector, i.e.,

$$h_{\text{edge}}(k) = v \cdot (k - ik_0), \quad (3)$$

where $k_0 = -\gamma(x)/v$. The shape of energy levels in complex energy space is a line, i.e., $\text{Re } E_{\text{edge}}(k) = v \cdot k$, and $\text{Im } E_{\text{edge}}(k) = \gamma$, as shown in Fig.1(b).

*Who has same contribution to this work

†Electronic address: spkou@bnu.edu.cn

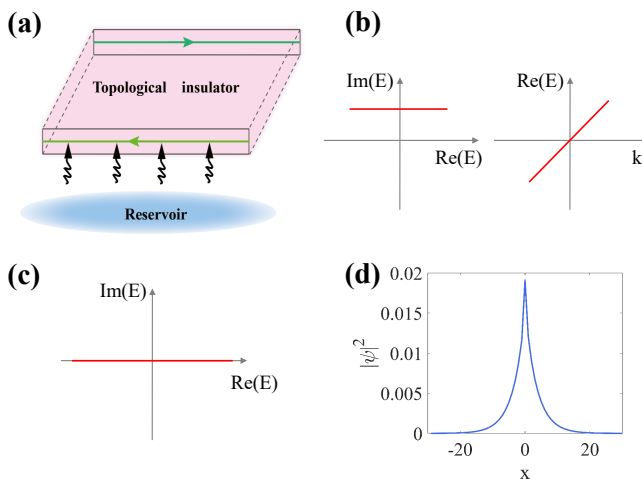


FIG. 1: (a) An example of a system with dissipative chiral modes: topological edge states of a two dimensional topological insulator with edge dissipation; (b) Energy levels in complex energy space and its dispersion relation under periodic boundary condition; (c) Energy levels in complex energy space under open boundary condition by considering a pair of gain/loss boundaries; (d) An illustration of chiral skin effect: one of topological edge states are localized around gain/loss boundary at $x = 0$.

In general, the one dimensional chiral modes are topological edge states on the boundary of a two dimensional (2D) topological insulator. However, because the boundary of a 2D topological insulator has no boundary, there doesn't exist usual open boundary condition for a chiral mode. Therefore, we define the open boundary condition (OBC) for 1D chiral modes with the help of the concept of "gain/loss boundary", which is a dissipation domain wall.

Definition – gain/loss boundary: gain/loss boundary is defined by a sign changing configuration of dissipation strength γ that separates the regions of gain and those of loss,

$$\text{sgn}(\gamma(x > 0)) \cdot \text{sgn}(\gamma(x < 0)) = -1. \quad (4)$$

What we need to emphasize is that the gain/loss boundary can be generalized to an interface between the regions of gain (or loss) and those of Hermitian regions. For example, if $\gamma \neq 0$ for the case of $x < 0$ and $\gamma = 0$ for the case of $x > 0$, this boundary is equivalent to having a gain/loss boundary at $x = 0$.

When there exist a pair of gain-loss boundaries with distance L , the boundary condition for edge states is defined as $\psi_{\text{edge}}(0) = \psi_{\text{edge}}(L)$. As a result, by solving the Schrodinger equation, the eigenstates of edge states with E takes the form $\psi_{\text{edge}}(x) = e^{i\frac{E}{v}x} e^{-\frac{1}{v} \int_0^x \gamma(x') dx'}$. In this case, the eigenvalues of chiral modes must be real, i.e., $\text{Im} E = 0$, as shown in Fig.1(c). The edge states become localized near gain-loss boundaries. For the simple case of a uniform dissipation $\gamma(x) = \gamma$, the energy spectra for

chiral modes described by $\psi_{\text{edge}}(x) = e^{ikx \pm \xi x}$ are characterized by usual BZ described by k . The localization length is given by $\xi = \frac{1}{k_0} = \left| \frac{v}{\gamma} \right|$. See the illustration in Fig.1(d). This result leads to an interesting effect – *the existence of intrinsic non-Hermitian skin effect for dissipative chiral modes*. To emphasize the character of chiral modes, we call it "chiral skin effect". We show the detailed discussion in supplementary materials.

In addition, CSE is quite different from usual NHSE or higher-order NHSE for bulk states. It was known that for the existence of usual NHSE or higher-order NHSE for bulk states is described by point-like topology configuration in complex energy space. One can define a winding number to characterize whether the existence of NHSE or not[29]. According to above discussion and Fig.1(b), one can see that for CSE there doesn't exist such point-like topology configuration in complex energy space. Instead, the energy levels for chiral modes with CSE is also a line, rather than a closed loop. In the following parts, we point out that CSE can be regarded as *fractional NHSE*.

By using an effective model in continuum limit to describe CSE, it is founded that CSE can occur in a system with dissipative chiral modes on gain/loss boundary. In summary, we have,

$$\text{Chiral modes} + \text{Dissipation} \rightarrow \text{Chiral skin effect}.$$

This conclusion can be naturally applied to the topological protected edge states in 2D topological insulators with dissipation.

Model Hamiltonian for non-Hermitian Haldane model with edge dissipation. Haldane model is a typical model of 2D topological insulator. To illustration the property of CSE, we consider Haldane model[42, 43] with dissipative edge, which has a periodic boundary condition (PBC) along x direction, and an OBC along y direction. See the illustration in Fig.2(a), of which only the lower (zigzag) edge is dissipative. The Hamiltonian of such a non-Hermitian Haldane model with edge dissipation is written as

$$\hat{H}_{\text{total}} = \hat{H}_{\text{haldane}} + i\gamma \sum_{\text{lower-edge}} c_i^\dagger c_i. \quad (5)$$

and

$$\hat{H}_{\text{haldane}} = t_1 \sum_{\langle ij \rangle} c_i^\dagger c_j + t_2 \sum_{\langle\langle ij \rangle\rangle} e^{i\phi_{ij}} c_i^\dagger c_j \quad (6)$$

where c_i^\dagger and c_i are creation and annihilation operators for a particle at the i -th site, respectively. $\langle i, j \rangle$ and $\langle\langle i, j \rangle\rangle$ denote the nearest-neighbor (NN) hopping and the next-nearest-neighbor (NNN) hopping, and t_1 and t_2 are the NN hopping and the NNN hopping strengths, respectively. $e^{i\phi_{ij}}$ is a complex phase into the NNN hopping, and we set the direction of the positive phase is clockwise ($|\phi_{ij}| = \frac{\pi}{2}$). The second term in Eq.(5) denotes dissipation. In this paper, we set to t_2 be constant, i.e., $t_2 \equiv 0.2t_1$.

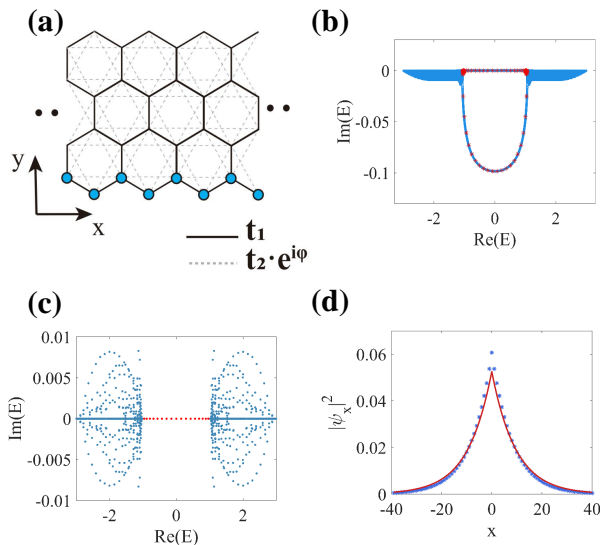


FIG. 2: (a) The illustration of Haldane model with edge dissipation. We add uniform imaginary potential on one of zigzag edges. (b) and (c) are the energy levels in complex energy space under PBC and those under OBC, respectively. Here, we set $\gamma = 0.1t_1$; (d) An illustration of chiral skin effect of topological edge states that are localized on gain/loss boundaries for the case of $\gamma = 0.1t_1$. The numerical results (blue stars) and the theoretical results (red lines) are consistent with each other.

In the following parts, we discuss the NHSE in three cases: the case with weak dissipation, the case with strong dissipation, and the case with intermediate dissipation, respectively.

Non-Hermitian skin effect for the case of weak dissipation – chiral skin effect. For the case of weak dissipation $\gamma \ll 1$, the dissipation term can be regarded as a perturbative term to original Hermitian Haldane model. Now, the topological protected edge states become dissipative chiral modes. According to above discussion, there must exist CSE. This is the *correct* mechanism for hybrid skin-topological effect. A detailed discussion of this conclusion is shown below.

Firstly, we consider the topological edge states for the Hermitian Haldane model \hat{H}_{Haldane} . Now, the effective single-body Hamiltonian of topological edge states $h_{\text{edge}}(k_x)$ becomes $h_{\text{edge}}(k_x) = \pm v_{\text{eff}} \cdot \sin(k_x - \pi)$ where v_{eff} characterizes the speed of topological edge states. We then denote the wave functions of topological edge states (or the chiral modes) to be $\psi_{\text{edge}}(x, y)$.

Secondly, we consider the effect of Haldane model with a weak dissipative edge \hat{H}_{total} . Now, the effective Hamiltonian of topological edge states becomes

$$h_{\text{edge}}(k_x) = \pm v_{\text{eff}} \cdot \sin(k_x - \pi) + i\gamma_{\text{eff}}(k_x) \quad (7)$$

where $\gamma_{\text{eff}}(k_x) = \langle \psi_{\text{edge}}(k_x) | \hat{H}_{\text{total}} | \psi_{\text{edge}}(k_x) \rangle$ is the effective dissipation. In Fig.2(b) and Fig.2(c), we plot the energy levels in complex energy space under PBC

and those under OBC, respectively. In addition, we do numerical calculation to verify our prediction. One can see that the numerical results (red stars) match our analytical results (blue lines inside real energy gap) very well. One can see that results from effective Hamiltonian $h_{\text{edge}}(k_x)$ match those from numerical calculations. In continuous limit, near $k_x = \pi$, $h_{\text{edge}}(k_x)$ is reduced into Eq.(3), i.e.,

$$h_{\text{edge}}(k_x) \simeq \pm v_{\text{eff}} \cdot (\Delta k \mp i\gamma_{\text{eff}}(k_x = \pi)/v) \quad (8)$$

where $\Delta k = k_x - \pi$. Thirdly, we discuss CSE. By considering a pair of gain/loss boundary on the dissipative edge, we have an open boundary condition for topological edge states (or the chiral modes). According to above discussion, for the topological edge states we have CSE with localization length about $\xi \sim \left| \frac{v_{\text{eff}}}{\gamma_{\text{eff}}(k_x = \pi)} \right|$. Fig.2(d) shows the CSE – topological edge states accumulate around the gain/loss boundary. In addition, we do numerical calculation to verify our prediction. One can see that the numerical results (blue stars) also match our analytical results (red lines) very well.

In addition, we point out that for both zigzag dissipative edge and armchair dissipative edge, we have the same CSE. This conclusion seems to conflict with previous results in Ref.[17]. In Ref.[17], it is claimed that there doesn't exist hybrid skin-topological effect for topological edge states on armchair edge for Haldane model with staggered bulk gain/loss. Let give a brief discussion on this conflict. For the Haldane model with armchair edge and staggered bulk gain/loss, the dissipation term is written as $i\gamma \sum_A c_i^\dagger c_i - i\gamma \sum_B c_i^\dagger c_i$. Now, for the case of weak dissipation, the effective single-body Hamiltonian for edge states becomes $h_{\text{edge}}(k_x) = \pm v_{\text{eff}} \cdot \sin(k_x - \pi) + i\gamma_{\text{eff}}$ where $\gamma_{\text{eff}} = \langle \psi_{\text{edge}}(k_x) | (i\gamma \sum_A c_i^\dagger c_i - i\gamma \sum_B c_i^\dagger c_i) | \psi_{\text{edge}}(k_x) \rangle$. One can see that for the armchair edge, due to the *symmetry* between A and B sub-lattice $\langle \psi_{\text{edge}}(k_x) | \sum_A c_i^\dagger c_i | \psi_{\text{edge}}(k_x) \rangle = \langle \psi_{\text{edge}}(k_x) | \sum_B c_i^\dagger c_i | \psi_{\text{edge}}(k_x) \rangle$, the effective dissipation strength γ_{eff} always disappears, i.e., $\gamma_{\text{eff}} = 0$; on the contrary, for the armchair edge, with the *symmetry* between A and B sub-lattice $\langle \psi_{\text{edge}}(k_x) | \sum_A c_i^\dagger c_i | \psi_{\text{edge}}(k_x) \rangle \neq \langle \psi_{\text{edge}}(k_x) | \sum_B c_i^\dagger c_i | \psi_{\text{edge}}(k_x) \rangle$ the effective dissipation strength γ_{eff} is finite, i.e., $\gamma_{\text{eff}} \neq 0$.

In summary, we conclude that *hybrid skin-topological effect comes from chiral skin effect* rather than certain NHSE on a one-dimensional chain or a higher-order non Hermitian skin effect.

Non-Hermitian skin effect for the case of strong dissipation – coexistence of chiral skin effect and usual non-Hermitian skin effect. For the case of strong dissipation $\gamma \rightarrow \infty$, the situation becomes complex. Now, there exist two types edge states – one is topological protected, chiral edge states, the other is non-topological, non-chiral edge states.

Firstly, we do numerical calculation for the case of $\gamma = 10t_1$ and show the results in Fig.3(a). Fig.3(a) shows

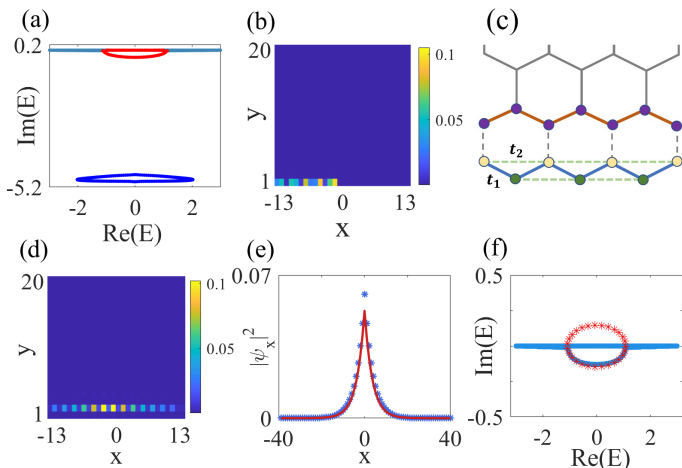


FIG. 3: (a) The energy levels in complex energy space. From it, one can see that inside the real energy gap, there are two types of energy levels – the curve with imaginary energy about γ just comes from non-topological, non-chiral edge states; the curve with imaginary energy about 0 comes from topological protected, chiral edge states; (b) An illustration of non-topological edge states. One can see that it locates on the dissipative edge; (c) Schematic of the effective double chain model for non-topological edge states that is cut from the original two dimensional Haldane model. Such model is really a generalized Tony-Lee model; (d) The illustration of topological edge states. This indicates that the dissipation pushes the topological edge states inward by one line; (e) CSE for topological edge states on the gain/loss boundaries (blue dotted lines), and NHSE for the corresponding Hatano-Nelson model (red lines); (f) The energy levels in complex energy space for topological edge states under PBC (open blue line in real energy gap) and those for 1D Hatano-Nelson model (closed dotted red lines). In this figure, we set $\gamma \equiv 10t_1$.

the energy levels in complex energy space. From it, one can see that inside the real energy gap, there are two types of energy levels – the blue curve with imaginary energy about γ just comes from non-topological, non-chiral edge states; the red curve with imaginary energy about 0 comes from topological protected, chiral edge states. Because the two types of edge states don't couple, we can discuss them one by one.

Secondly, we discuss the properties of non-topological, (non-chiral) edge states. According to Fig.3(b), one can see that under OBC by considering a pair of gain/loss boundaries the position of non-topological edge states is localized around gain/loss boundary and almost at $y_J = y_0$, where y_0 denotes the position of the dissipative edge. Therefore, to characterize the non-topological, non-chiral edge states, we can cut the outermost lattice sites to make up a quasi 1D double chain. See the illustration in Fig.3(c). In particular, we find that the effective Hamiltonian for a double chain model is a generalized Tony-Lee model[11]. Let us give a detailed discussion on this conclusion.

To completely recognize non-topological, non-chiral

edge state, the key point is obtaining its effective Hamiltonian $\hat{H}_{\text{non-top}}$. To obtain $\hat{H}_{\text{non-top}}$ from original Hamiltonian \hat{H}_{total} , we introduce projection operator $\hat{P}_{\text{non-top}}$, which projects the original Hamiltonian into the subspace of non-topological edge states. Under projection, in strong dissipation region, the perturbation theory for the non-topological states can be used by integrating out the bulk degree of freedom. Then, we obtain its effective Hamiltonian,

$$\begin{aligned} \hat{H}_{\text{non-top}} &= \hat{P}_{\text{non-top}} \hat{H}_{\text{total}} \hat{P}_{\text{non-top}} \\ &= \sum_{k_x \in (-\pi, \pi)} a_k^\dagger [t_2 \sigma_z \sin k_x \\ &\quad + t_1 \sigma_x (1 + \cos k_x) + t_1 \sigma_y \sin k_x \\ &\quad + i\gamma_{\text{non-top}} (\sigma_z + I) + i\gamma_{\text{eff}}] a_{k_x} \end{aligned} \quad (9)$$

where $a_{A/B, k_x}^\dagger = \hat{P}_{\text{non-top}} c_{A/B, k_x}^\dagger$ and $a_{A/B, k_x} = \hat{P}_{\text{non-top}} c_{A/B, k_x} \hat{P}_{\text{non-top}}$. Here, A and B denotes the A and B sublattices, respectively. $\gamma_{\text{non-top}} = \frac{t_2^2}{2\gamma}$ denotes the strength of effective mode-selective dissipation on non-topological edge states and γ_{eff} denotes the strength of uniform dissipation on non-topological edge states. The detailed calculations are provided in supplementary materials. This is just the generalized Tony-Lee model[11].

As discussing in above parts, there exists usual, non-chiral non-Hermitian skin effect. In Fig.3(b), we show the localization effect of non-topological edge states on the gain/loss boundaries. In Ref.[17], it was believed that the hybrid skin-topological effect comes from those on a one-dimensional chain with nonlocal flux. However, the truth is that *it is the non-topological edge states rather than the topological edge states that is characterized by a non-Hermitian model on a one-dimensional chain with nonlocal flux!*

Thirdly, we discuss the properties of topological, (chiral) edge states. Using similar approach, we can obtain the effective Hamiltonian for topological edge states for the case of strong dissipation $\gamma \rightarrow \infty$ as

$$\begin{aligned} \hat{H}_{\text{top}} &= \hat{P}_{\text{top}} \hat{H}_{\text{total}} \hat{P}_{\text{top}} \\ &= \sum_{k_x \in (-\pi/2, \pi/2)} b_{k_x}^\dagger (v_{\text{eff}} \sin k_x + i\gamma_{\text{top}}(k_x)) b_{k_x}, \end{aligned} \quad (10)$$

where $b_{k_x}^\dagger = \hat{P}_{\text{top}} c_{k_x}^\dagger \hat{P}_{\text{top}}$, and $b_{k_x} = \hat{P}_{\text{top}} c_{k_x} \hat{P}_{\text{top}}$. The projection operator \hat{P}_{top} projects the original Hamiltonian into the subspace of topological edge states. $\gamma_{\text{top}}(k_x)$ denotes the strength of effective dissipation for topological edge states. In particular, by data fitting for energy levels in complex energy space, we find that $\gamma_{\text{top}}(k_x)$ is almost proportional to $\cos k_x$, i.e.,

$$\gamma_{\text{top}}(k_x) = \zeta \cos k_x \quad (11)$$

where ζ is k_x -independent parameter that is determined by γ . In the limit of $\gamma \rightarrow \infty$, we have $\gamma_{\text{top}}(k_x) \rightarrow 0$.

According to Fig.3(d), one can see that the position of topological, chiral edge states has a maximum value at $y_J = y_0 - 1$, where y_0 denotes the position of the dissipative edge. This indicates that the dissipation pushes the topological edge states inward by one line.

In addition, we consider the NHSE for topological edge states. For the case of a pair of gain-loss boundaries, there again exists chiral skin effect. However, the chiral skin effect for the case of strong dissipation is much more exotic. According to \hat{H}_{top} , the effective Hamiltonian for the case of $\gamma = 10t_1$ looks like a 1D Hatano-Nelson model. To make it clear, we write down the corresponding Hamiltonian of the 1D Hatano-Nelson model that is

$$\begin{aligned} \hat{H}_{\text{HN}} &= \sum_i (t_L b_i^\dagger b_{i+1} + t_R b_{i+1}^\dagger b_i) \\ &= \sum_{k_x \in (-\pi, \pi)} b_{k_x}^\dagger (v_{\text{eff}} \sin k_x + i\zeta \cos k_x) b_{k_x} \end{aligned} \quad (12)$$

where $t_L = (v_{\text{eff}} - \zeta)/2$ and $t_R = (v_{\text{eff}} + \zeta)/2$. For example, for the case of $\gamma = 10t_1$ we have $t_L = 0.6181t_1$, and $t_R = 0.4709t_1$. Due to CSE, we show the localization effect of topological edge states on the gain/loss boundaries in Fig.3(e), of which the red lines denote the NHSE for $\hat{H}_{\text{HN}} = \sum_i (t_L b_i^\dagger b_{i+1} + t_R b_{i+1}^\dagger b_i)$ and the blue dotted lines denote CSE for topological edge states of 2D Haldane model with dissipative edge for the case of $\gamma = 10t_1$. The results from models match. However, due to $k_x \in (-\pi/2, \pi/2)$ rather than $k_x \in (-\pi, \pi)$, the effective Hamiltonian of topological edge states is only *1D half Hatano-Nelson model*. Therefore, the energy levels in complex energy space for topological edge states under PBC (open blue line in real energy gap) is also half of those of a 1D Hatano-Nelson model (closed dotted red lines), i.e., the half with positive imaginary parts $\text{Im} E_{k_x} > 0$ or the half with positive imaginary parts $\text{Im} E_{k_x} < 0$. See the illustration in Fig.3(f). Therefore, we call chiral skin effect to be *fractional non-Hermitian skin effect*.

In summary, we found that for the case of strong dissipation, chiral skin effect for topological edge states and usual non-Hermitian skin effect for non-topological edge states *coexist*.

Non-Hermitian skin effect for the case of intermediate dissipation – Hybrid skin effects for edge states and its phase transitions. According to above discussion, we found that for the case of strong dissipation, there exist two types of edge states – topological edge states and non-topological edge states. For the case of intermediate dissipation, the situation becomes much more complex. The two types of edge states couple and correspondingly the two types of non-Hermitian skin effects hybrid that leads to an additional type of non-Hermitian skin effect – *hybrid skin effect*.

Now, the effective Hamiltonian for both edge states turns into

$$\hat{H}_{\text{edge}} = \hat{H}_{\text{non-top}} + \hat{H}_{\text{top}} + \hat{H}_{\text{coupling}} \quad (13)$$

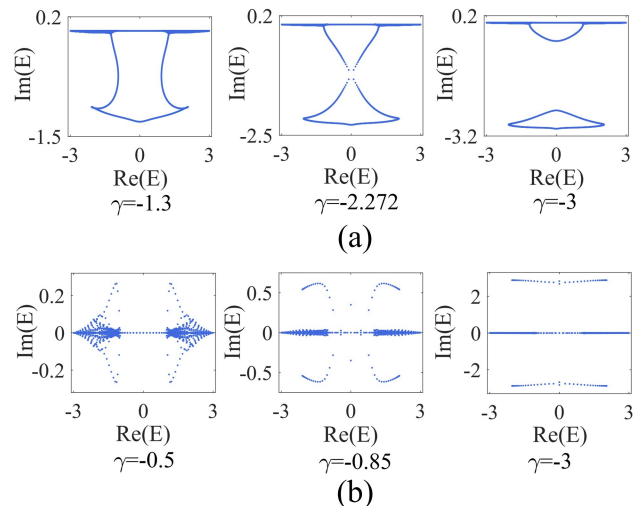


FIG. 4: (a) The evolution of energy levels in complex energy space for the edge states under periodic boundary condition in Haldane model via the strength γ of edge dissipation. A hybridization phase transition at $\gamma = -2.272t_1$ that is a PT symmetry breaking; (b) The evolution of energy levels in complex energy space for the edge states under open boundary condition by considering a pair of gain/loss boundaries in Haldane model via the strength γ of edge dissipation. A hybridization phase transition at $\gamma = -0.85t_1$ that is a PT symmetry breaking.

where $\hat{H}_{\text{coupling}}$ are couplings between bulk states, non-topological edge states and topological edge states that is written as

$$\hat{H}_{\text{coupling}} = \sum_{k_x \in (-\pi, \pi)} b_{k_x/2}^\dagger \lambda_{k_x} a_{k_x} + h.c \quad (14)$$

where $\lambda_{k_x} = \langle \psi_{\text{non-top}}(k_x) | \hat{H}_{\text{total}} | \psi_{\text{top}}(k_x) \rangle$ denotes the coupling strength.

An interesting phenomenon is a *hybridization phase transition* between non-topological edge states and topological edge states.

For the case of PBC, as shown in the area of $\gamma > \gamma_c$ in Fig.4(a), the loops in complex energy spectrum for non-topological edge states and those for topological edge states are well separated, which means that there are not hybridization. On the other hand, as shown in the area of $\gamma < \gamma_c$ in Fig.4(a), when the coupling between non-topological edge states and topological edge states is large enough, loops for non-topological edge states and those for topological edge states are reconstructed and turn into a big one, which means the non-topological modes and the topological modes become hybridized together.

Let us give an analytical explanation on the hybridization phase transition from above effective model for edge states. Due to the inversion symmetry for effective model for edge states, the hybridization phase transition is characterized by gap closing at high symmetry point, $k_x = \pi$. At $k_x = \pi$, the energy levels

are $i\gamma_{\text{non-top}}$, and $i\gamma_s/2 \pm \sqrt{\lambda_{k=\pi}^2 - (\gamma_{s,\text{PBC}}/2)^2}$ where $\gamma_{s,\text{PBC}} \equiv \gamma_{\text{non-top}} - 2\gamma_{\text{eff}} - \gamma_{\text{top}}(\pi)$. In particular, the hybridization phase transition at $\gamma_{s,\text{PBC}} = 2\lambda_{k=\pi}$ is a PT phase transition. At the EP, one of the non-topological edge state merges into the topological edge state at $k = \pi$. The detailed calculations is provided in supplementary materials.

For the case of OBC by considering a pair of gain-loss boundaries, there also exists a hybridization phase transition between non-topological edge states and topological edge states, As shown in Fig.4(b). We denote the critical point to be $\gamma_{c,\text{OBC}}$. In general, the critical point under OBC $\gamma_{c,\text{OBC}}$ is different from that under PBC $\gamma_{s,\text{PBC}} = 2\lambda_{k=\pi}$. This phenomenon of the shifting of critical points under OBC and those under PBC is similar to the breakdown of bulk-boundary correspondence in topological insulator due to usual NHSE for bulk states. In the phase of $\gamma_{s,\text{OBC}} > \gamma_{c,\text{OBC}}$, there is no hybridization between non-topological and topological edge states. The localization length of chiral skin effect for topological edge states and that of usual non-Hermitian skin effect for non-topological edge states are different. Therefore, the chiral skin effect and usual non-Hermitian skin effect become independent; when $\gamma_{s,\text{OBC}} < 2\lambda_{k=\pi}$, the non-topological edge states and the topological edge states become hybridized. The localization length of chiral skin effect for topological edge states and that of usual non-Hermitian skin effect for non-topological edge states are same.

Non-local non-Hermitian skin effect and the possible boundary/edge reconstruction. In this part, we discuss the interplay between the topological edge states on both edges (the edge with dissipation and that without). To avoid the effect from non-topological edge states, we consider the case with large dissipation. Now, there is no hybridization between non-topological and topological edge states.

We then consider a Haldane model on a strip, of which one edge has dissipation, but the other hasn't. The distance between two edges is set to be L_y . See the illustration in 5(a).

Firstly, we consider the case of PBC. Now, the effective Hamiltonian of topological edge states on both edges is obtained as

$$\begin{aligned} \hat{H}_{\text{top}} = & \sum_{k_x} b_{k_x}^\dagger (t_1 \sin k_x + i\gamma_{\text{top}}(k_x)) b_{k_x} \\ & - \sum_{k_x} f_{k_x}^\dagger (t_1 \sin k_x) f_{k_x} + \sum_{k_x} f_{k_x}^\dagger \Delta_{k_x} b_{k_x} + h.c., \end{aligned} \quad (15)$$

where $f_{k_x}^\dagger$ and f_{k_x} are electric operators on the edge without dissipation and Δ_k is tunneling strength between two edges. As a result, the energy levels are $E_k = i\gamma_{\text{top}}(k_x)/2 \pm \sqrt{(t_1 \sin k_x + i\gamma_{\text{top}}(k_x)/2)^2 + (\Delta_{k_x})^2}$. When L_y is very small, the topological edge states on both edges couple. On the contrary, in limit of $L_y \rightarrow \infty$ (for example $L = 20$), $\Delta_k \rightarrow 0$, we have $E_k \rightarrow -t_1 \sin k$

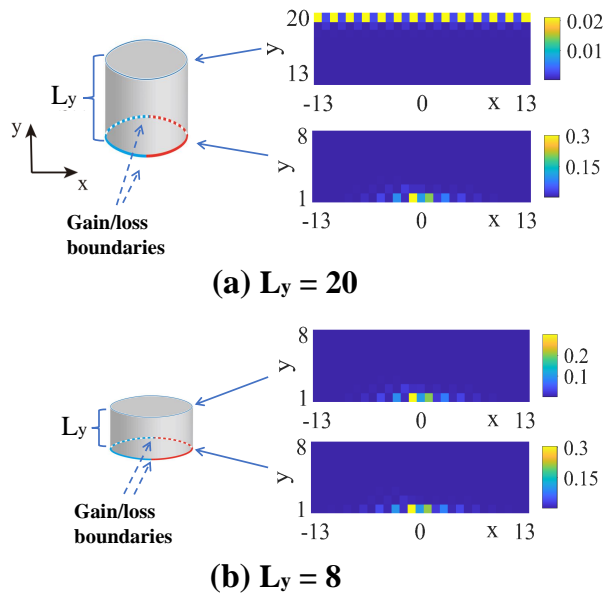


FIG. 5: The phenomenon of boundary reconstruction: the illustration of topological edge states for OBC by considering gain/loss boundary on one edge and PBC for the other without dissipation. (a) $L_y = 20$; (b) $L_y = 8$. In (a), the topological edge states on dissipative edge are localized on the gain/loss boundary of the corresponding edge, the other on dissipationless edge are extended on its corresponding edge; In (b), both topological edge states on both edge are localized on the gain/loss boundary of same edge.

on one edge and $E_k \rightarrow t_1 \sin k_x + i\gamma_{\text{top}}(k_x)$ on the other).

Secondly, we consider the case of OBC by considering gain/loss boundary on one edge. In the limit of $L_y \rightarrow \infty$ (for example $L_y = 15$), the results are similar to those under PBC. See the results in Fig.5(a). A very *strange* phenomenon occurs when L_y is small (for example $L_y = 5$). See Fig.5(b). *Both the topological edge states on the edge with dissipation and those on the edge without dissipation all localize on the gain/loss boundary.* To emphasize the results, we call it *non-local non-Hermitian skin effect*. It is obvious that the non-local non-Hermitian skin effect cannot be described by usual effective Hamiltonian such like \hat{H}_{top} . Until now, the mechanism of non-local non-Hermitian skin effect is still a mystery. We guess that this effect can be understood by a new phenomenon of *boundary/edge reconstruction* – for the small L case, the gain/loss boundary may open a new channel (or boundary) from one edge to the other. In the future, will study this open question and try to give a reasonable answer.

Conclusion. In this paper, we found a new type of NHSE named CSE – NHSE for dissipative chiral modes. By applying the idea of CSE, hybrid topological skin effect is finally perfectly explained: according to CSE, when topological edge states of a 2D topological insulator become dissipative, they become dissipative chiral modes and then there exists CSE. Therefore, under OBC by considering gain/loss boundaries, these topological edge

states accumulate and become localized on the gain/loss boundaries. In addition, an unexpected effect – non-local non-Hermitian skin effect is discovered, which leads to topological edge states on both sides turn to localize only on gain/loss boundary of same edge.

In the future, we will study the CSE for topologi-

cal edge states in other types of topological quantum states, such as higher order topological insulator, topological superconductors, topological semi-metal. Then, we try to systematically understand the interplay of non-Hermitian physics and topological quantum states.

-
- [1] C. M. Bender and S. Boettcher, Real Spectra in Non-Hermitian Hamiltonians Having PT Symmetry, *Phys. Rev. Lett.* **80**, 5243-5246 (1998).
- [2] H. Shen, B. Zhen, and L. Fu, Topological Band Theory for Non-Hermitian Hamiltonians, *Phys. Rev. Lett.* **120**, 146402 (2018).
- [3] T. Liu, Y. R. Zhang, Q. Ai, Z. Gong, K. Kawabata, M. Ueda, and F. Nori, Second-Order Topological Phases in Non-Hermitian Systems, *Phys. Rev. Lett.* **122**, 076801 (2019).
- [4] X. W. Luo and C. Zhang, Higher-Order Topological Corner States Induced by Gain and Loss, *Phys. Rev. Lett.* **123**, 073601 (2019).
- [5] C. X. Guo, X. R. Wang, C. Wang, and S. P. Kou, Defective edge states and number-anomalous bulk-boundary correspondence in non-Hermitian topological systems, *Phys. Rev. B* **101**, 144439 (2020).
- [6] N. Matsumoto, K. Kawabata, Y. Ashida, S. Furukawa, and M. Ueda, Continuous Phase Transition without Gap Closing in Non-Hermitian Quantum Many-Body Systems, *Phys. Rev. Lett.* **125**, 260601 (2020).
- [7] F. Yang, H. Wang, M. L. Yang, C. X. Guo, X. R. Wang, G. Y. Sun, and S. P. Kou, Hidden Continuous Quantum Phase Transition without Gap Closing in Non-Hermitian Transverse Ising Model, *New J. Phys.* **24**, 043046 (2022).
- [8] W. Wang and Z. Ma, Concurrence of anomalous Hall effect and charge density wave in a superconducting topological kagome metal, *Phys. Rev. B* **106**, 115306 (2022).
- [9] E. J. Bergholtz, J. C. Budich, and F. K. Kunst, Exceptional topology of non-hermitian systems, *Rev. Mod. Phys.* **93**, 015005 (2021).
- [10] Y. Ashida, Z. Gong, and M. Ueda, Non-Hermitian Physics, *Advances in Physics* **69**, 249 (2020).
- [11] T. E. Lee, Anomalous Edge State in a Non-Hermitian Lattice, *Phys. Rev. Lett.* **116**, 133903 (2016).
- [12] W. D. Heiss, The physics of exceptional points, *Journal of Physics A: Mathematical and Theoretical* **45**, 444016 (2012).
- [13] S. Yao and Z. Wang, Edge States and Topological Invariants of Non-Hermitian Systems, *Phys. Rev. Lett.* **121**, 086803 (2018).
- [14] K. Yokomizo and S. Murakami, Non-Bloch Band Theory of Non-Hermitian Systems, *Phys. Rev. Lett.* **123**, 066404 (2019).
- [15] C. H. Lee and R. Thomale, Anatomy of skin modes and topology in non-Hermitian systems, *Phys. Rev. B* **99**, 201103 (2019).
- [16] X. R. Wang, C. X. Guo, Q. Du, and S. P. Kou, State-Dependent Topological Invariants and Anomalous Bulk-Boundary Correspondence in Non-Hermitian Topological Systems with Generalized Inversion Symmetry, *Chinese Physics Letters* **37**, 117303 (2020).
- [17] Y. Li, C. Liang, C. Wang, C. Lu and Y. C. Liu, Gain-Loss-Induced Hybrid Skin-Topological Effect, *Phys. Rev. Lett.* **128**, 223903 (2022).
- [18] C. H. Lee, L. Li, and J. Gong, Hybrid Higher-Order Skin Topological Modes in Non-Reciprocal Systems, *Phys. Rev. Lett.* **123**, 016805 (2019).
- [19] S. Yao, F. Song, and Z. Wang, Non-Hermitian Chern Bands, *Phys. Rev. Lett.* **121**, 136802 (2018).
- [20] F. K. Kunst, E. Edvardsson, J. C. Budich, and E. J. Bergholtz, Biorthogonal Bulk-Boundary Correspondence in Non-Hermitian Systems, *Phys. Rev. Lett.* **121**, 026808 (2018).
- [21] C. Yin, H. Jiang, L. Li, R. Lü, and S. Chen, Geometrical meaning of winding number and its characterization of topological phases in one-dimensional chiral non-Hermitian systems, *Phys. Rev. A* **97**, 052115 (2018).
- [22] K. Kawabata, K. Shiozaki, and M. Ueda, Anomalous helical edge states in a non-Hermitian Chern insulator, *Phys. Rev. B* **98**, 165148 (2018).
- [23] Y. Xiong, Why does bulk boundary correspondence fail in some non-hermitian topological models, *J. Phys. Commun.* **2**, 035043 (2018).
- [24] V. M. Martinez Alvarez, J. E. Barrios Vargas, L. E. F. Foa Torres, Non-Hermitian robust edge states in one dimension: Anomalous localization and eigenspace condensation at exceptional points, *Phys. Rev. B* **97**, 121401(R) (2018).
- [25] A. Ghatak and T. Das, New topological invariants in non-Hermitian systems, *J. Phys.: Condens. Matter* **31**, 263001 (2019).
- [26] K. Yokomizo and S. Murakami, Non-Bloch Band Theory of Non-Hermitian Systems, *Phys. Rev. Lett.* **123**, 066404 (2019).
- [27] S. Longhi, Probing non-Hermitian skin effect and non-Bloch phase transitions, *Phys. Rev. Research* **1**, 023013 (2019).
- [28] F. Song, S. Yao, and Z. Wang, Non-Hermitian Skin Effect and Chiral Damping in Open Quantum Systems, *Phys. Rev. Lett.* **123**, 170401 (2019).
- [29] K. Zhang, Z. Yang, and C. Fang, Correspondence between Winding Numbers and Skin Modes in Non-Hermitian Systems, *Phys. Rev. Lett.* **125**, 126402 (2020).
- [30] S. Mu, C. H. Lee, L. Li, and J. Gong, Emergent Fermi surface in a many-body non-Hermitian fermionic chain, *Phys. Rev. B* **102**, 081115(R) (2020).
- [31] E. Lee, H. Lee, and B. Yang, Many-body approach to non-Hermitian physics in fermionic systems, *Phys. Rev. B* **101**, 121109 (2020).
- [32] T. Liu, J. J. He, T. Yoshida, Z. L. Xiang, and F. Nori, Non-Hermitian topological Mott insulators in one-dimensional fermionic superlattices, *Phys. Rev. B* **102**, 235151 (2020).
- [33] W. W. Zhu and J. B. Gong, Hybrid skin-topological modes without asymmetric couplings, *Phys. Rev. B* **106**,

- 035425 (2022).
- [34] D. W. Zhang, Y. L. Chen, G. Q. Zhang, L. J. Lang, Z. Li, and S. L. Zhu, Skin superfluid, topological Mott insulators, and asymmetric dynamics in an interacting non-Hermitian Aubry-André-Harper model, *Phys. Rev. B.* **101**, 235150 (2020).
- [35] Z. Xu and S. Chen, Topological Bose-Mott insulators in one-dimensional non-Hermitian superlattices, *Phys. Rev. B.* **102**, 035153 (2020).
- [36] D. S. Borgnia, A. J. Kruchkov, and R. J. Slager, Non-Hermitian Boundary Modes and Topology, *Phys. Rev. Lett.* **124**, 056802 (2020).
- [37] Y. Yi and Z. Yang, Non-Hermitian Skin Modes Induced by On-Site Dissipations and Chiral Tunneling Effect, *Phys. Rev. Lett.* **125**, 186802 (2020).
- [38] N. Okuma and M. Sato, Non-Hermitian Skin Effects in Hermitian Correlated or Disordered Systems: Quantities Sensitive or Insensitive to Boundary Effects and Pseudo-Quantum-Number, *Phys. Rev. Lett.* **126**, 176601 (2021).
- [39] F. Roccati, Non-Hermitian skin effect as an impurity problem, *Phys. Rev. A.* **104**, 022215 (2021).
- [40] K. Zhang, Z. Yang and C. Fang, Universal non-Hermitian skin effect in two and higher dimensions, *Nat. Commun.* **13**, 2496 (2022).
- [41] K. Yokomizo and S. Murakami, Non-Bloch bands in two-dimensional non-Hermitian systems, arXiv:2210.04412.
- [42] F. D. M. Haldane, Model for a Quantum Hall Effect without Landau Levels: Condensed-Matter Realization of the "Parity Anomaly", *Phys. Rev. Lett.* **61**, 2015 (1988).
- [43] G. Jotzu, M. Messer, R. Desbuquois, M. Lebrat, T. Uehlinger, D. Greif, and T. Esslinger, Experimental realization of the topological Haldane model with ultracold fermions, *Nature.* **515**, 237 (2014).